



Optimization of Electromagnetic Band Gap Structure for Mutual Coupling Reduction in Antenna Arrays-A Comparative Study

K. Praveen Kumar^{1*}, Habibullah Khan²

¹Lecturer, Dept. of Electrical and Electronics Engineering, Eritrea Institute of Tech., Mainafhi, State of Eritrea, East Africa.

²Professor, Dept. of ECE, KL Deemed to be University, Vaddeswaram, A.P, India.

*Corresponding author E-mail: kpraveenkumar24817@gmail.com

Abstract

In this paper, two new three layer (stacked) Electromagnetic Band Gap structures are proposed, named as Stacked Electromagnetic Band Gap (SEBG) and Progressive Stack Electromagnetic Band Gap (PSEBG) structures. Its electromagnetic (EM) properties are determined by using Finite element method (FEM) based simulator and obtained results are compared with classical mushroom type electromagnetic band gap (MEBG) structure. Both SEBG and PSEBG structures proposed in this paper consists of two layers above the conducting ground plane; a lower layer, contains array of small MEBGs with square patches and an upper layer contains square planar MEBG structure. Vertical conducting stubs passing through substrate shorting all square patches in both the layers with conducting ground. Three EBG structures are exhibiting the property of forbidden band gap (FBG), where surface wave propagation is restricted. The FBG property helps in minimization of mutual coupling between array antennas when electromagnetic band gap structures are incorporated between array elements. In this paper, the level of coefficient of mutual coupling between array antenna in the presence of SEBG and PSEBG are investigated, obtained results are compared with classical MEBG results. The co-efficient of mutual coupling is reduced up to 12dB in the presence of proposed models.

1. Introduction

The microstrip patch antennas are arranged in an array, for high gain, beam steering [1] applications. Array architecture of consists of multiple number of antenna elements printed on common substrate. This may cause mutual coupling between antenna elements because of excitation of surface waves, space waves and overlapping of near fields between the array elements. This results in reduction of antenna performance in terms of antenna gain, operational bandwidth and radiation efficiency as well as overall system performance [2]. Practically, the coupling mechanisms depend on several factors such as permittivity and thickness of substrate material, ground plane size, type of excited modes etc. [3]. In generally, physical distance between the antenna elements is maintained half an operating wave length to reduce mutual coupling [4]. Various techniques have been proposed in literature to reduce the mutual coupling between array elements such as: corrugations [5,6], split ring resonators (SRR) [7,8] and Defected Ground Structures (DGS)[9-11]. In [12] MEBG is proposed and applied to improve the isolation of radiating elements in an array by suppressing the surface wave propagation. Various EBG architectures were designed [13-19] and applied to antenna arrays for mutual coupling reduction. In this paper, MEBG surface have been chosen as a base of designing new SEBG and PSEBG surfaces. Both the structures consists of three layers; top layer contains square planar MEBG unit cell, lower layer (middle or hidden layer) contains small square array of MEBG unit cells and bottom layer contains a plane conducting sheet, all the patches are shorted to plane conducting sheet at bottom layer by vertical

conducting stubs centrally to the patches through FR4 substrate. The overall size and individual particles of proposed SEBG and PSEBG unit cells are small compared to its operating wavelength. The shape and dimension of individual elements of unit cell plays key role for synthesis of its frequency response, FBG and AMC properties. The FBG property of EBG unit cell permits no surface propagation. The surface wave propagation between antenna elements is root cause for mutual coupling so by introduction of EBGs between array elements one can reduce the co-efficient of mutual coupling or improvise the isolation.

The objective of this paper is to introduce two new electromagnetic band gap structures named as SEBG, PSEBG and determine its efficiency in reducing coefficient of mutual coupling in antenna arrays. The first part of the paper contains design procedure of SEBG and PSEBG structures and their emerging from fundamental MEBG is explored and its FBG property is determined using FEM based simulator. In second part, the level of coefficient of mutual coupling between E-plane array antenna by the introduction of new SEBG and PSEBG is studied and obtained results are compared with the results of MEBG model.

2. Unit Cell Design

Figure 1 to 3 showing the schematic diagrams of MEBG, SEBG and PSEBG. The MEBG is considered here as reference structure. All EBG models are designed on FR4 substrate, relative permittivity of 4.4, permeability of 1 and loss tangent of 0.02 with a thickness (height) 'H' of 3.2mm (124mil). The lattice in Figure 1 consists of square metal patch of 17.5X17.5 mm² printed on one

top side of FR4 substrate backed continuous ground plane. A vertical conducting stub (via) of radius 0.475mm, is used to short the square metal patch with conducting ground through substrate from their center. The lattice in figure 2 consists of square metal patches arranged in layers (stacked), where lower layer contains array of four compact square metal patches having a dimension of $3.4 \times 3.4 \text{ mm}^2$ mounted at a height $H/2$ of 1.6mm (62mil), placed at four corners of UC, top layer contains planar square metal patch of size $17.5 \times 17.5 \text{ mm}^2$, placed at a height of 3.2mm. All these patches are connected to ground plane lying on the other side of substrate by a vertical conducting stub of radius of 0.475mm from their center. The lattice in figure 3 consists of vertically stacked arrangement of patches, where lower layer contains progressive array of compact square metal patches, the array of square patches placed at four corners of a UC having dimensions of $3.4 \times 3.4 \text{ mm}^2$. Next array of square patches placed diagonally with a size of $3.075 \times 3.075 \text{ mm}^2$. All these patches are placed at a height $H/2$ of 1.6mm (62mil), connected to ground plane lying on the other side of substrate by a conducting vertical stub of radius 0.475mm from their center. Top layer is similar to what is explained in figure 2. In this study, to minimize EBG cell size, the researcher has chosen FR4 with thickness 3.2mm otherwise, the AMC metallization will get excited by the feed line similar to an antenna if EBG UC size is equal or greater than the radiating patches. The summary of complete dimensions of all three (MEBG, SEBG and PSEBG) models are listed in table I.

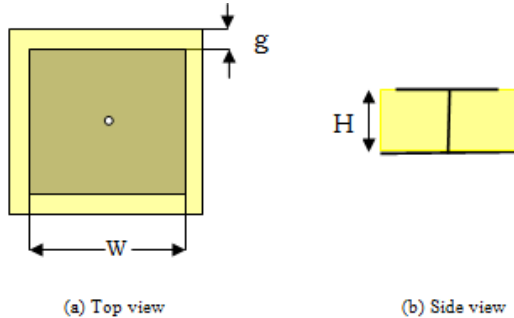


Fig. 1: Schematic of MEBG unit cell printed on FR4 substrate contains square patch on top face, vertical conducting stub and ground conductor on back face.

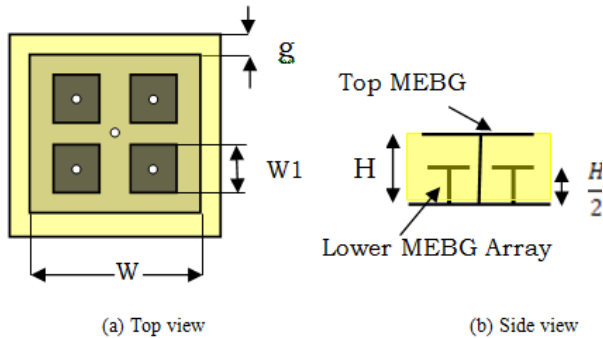


Fig. 2: Schematic of SEBG unit cell printed on FR4 substrate contains planar square patch on top face, array of square patches in the middle layer ground conductor on back face and vertical conducting stubs passing through the substrate shorting all square patches in both the layers to ground conductor.

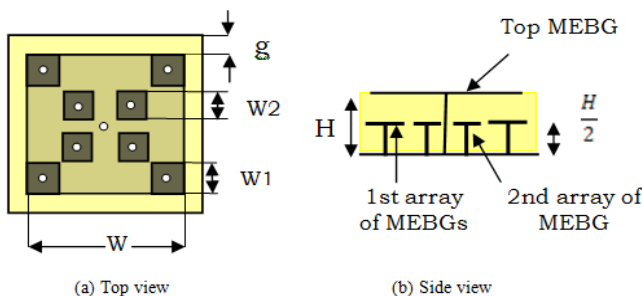


Fig. 3: Schematic of PSEBG unit cell printed on FR4 substrate contains planar square patch on top face, array of square patches in the middle layer ground conductor on back face and vertical conducting stubs passing through the substrate shorting all square patches in both the layers to ground conductor.

Table I: Dimensions of all Three UCs of Electromagnetic Band Gap Structures

Parameter Name	Symbol	MEBG	SEBG	PSEBG
Square patches	W X W	17.5X17.5 mm ²	17.5X17.5 mm ²	17.5X17.5 mm ²
	W1 X W1		3.4X3.4 mm ²	3.4X3.4 mm ²
	W2 X W2			3.075X3.075 mm ²
Gap	G	1mm	1mm	1mm
Stub radius	R	0.475mm	0.475mm	0.475mm
Dielectric substrate height	H	3.2mm	3.2mm	3.3mm

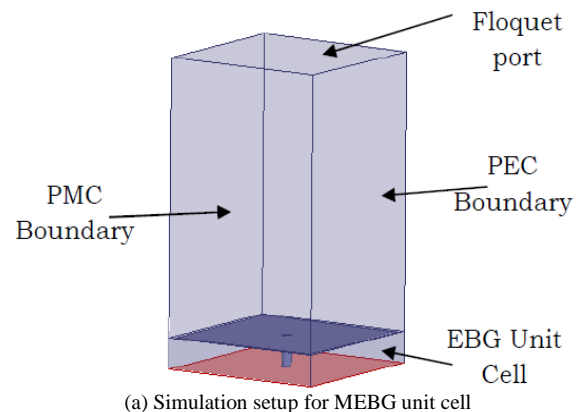
The MEBG, SEBG and PSEBG UC dimensions such as height of substrate, patch size, gap between adjacent patches and substrate material are considered identical, so that their resonance frequency will be remain constant and equal and other important properties such as AMC and FBG can be easily compared.

3. Analysis of EBG Structures

Numerous methodologies are available in literature for the analysis of EBG UC. They are broadly classified into four categories [20]: 1) Lumped element circuit model [12], 2) Transmission line model [21], 3) Computational electromagnetic modeling using of full wave solvers. Due to the complexity of the electromagnetic band gap structures, it is usually difficult to characterize them with above specified two analytical methods. Full wave electromagnetic simulators that are based on advanced numerical methods are popularly used in analysis of electromagnetic band gap structures. In this paper reflection phase, high impedance region and dispersion features of MEBG, SEBG and PSEBG are determined by using FEM based 3D-EM simulator.

AMC Behavior Analysis

AMC is one of the unusual but important properties of the electromagnetic band gap structures. To determine the AMC property of three models, FEM simulation based on the Bloch-Floquet theory (High Frequency Structure simulator (HFSS) from Ansoft) is considered. In the FEM simulator, to determine the coefficient of reflection phase, the UC should be applied with perfect magnetic conductor (PMC) and perfect electric conductor (PEC) boundaries periodically on its four sides. To model the effect of periodic replication in an infinite array structure, the wave port on the top face of UC is de-embedded, the complete simulation setup is shown in Figure 4.



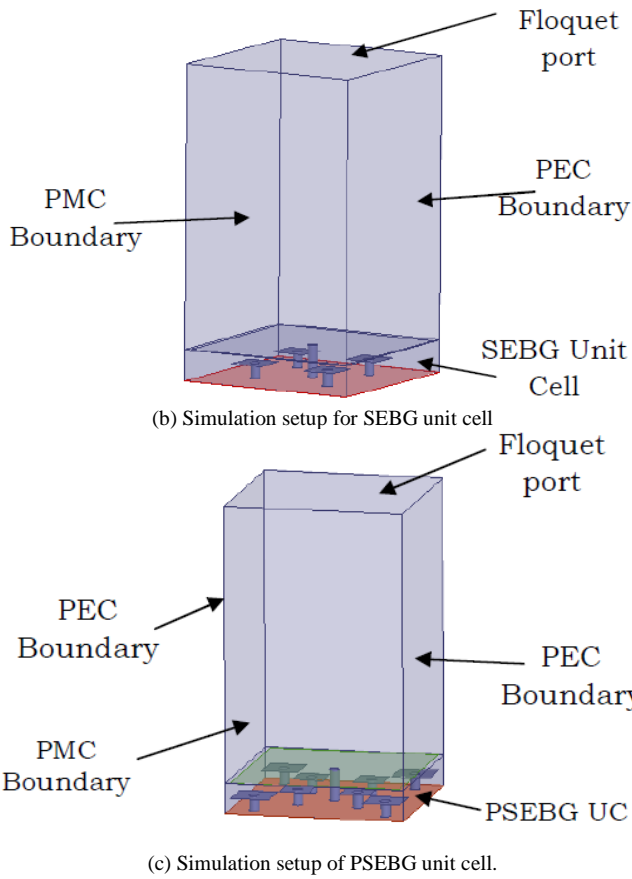


Fig. 4: AMC property measurement setup of MEBG, SEBG and PSEBG unit cells in FEM based 3D-EM simulator contains periodic boundaries on its four sides with topped wave port.

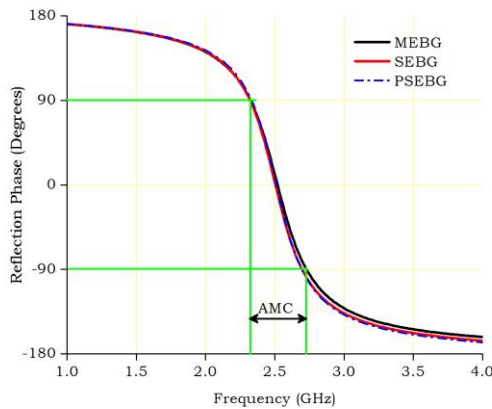


Fig. 5: Reflection phase diagram, represents the in-phase band gap and resonating frequency of respective unit cell.

Figure 5 shows the coefficient of reflection phase for the normal incident plane waves for MEBG, SEBG and PSEBG structures. It varies continuously from $+180^{\circ}$ to -180° relative to the frequency. The frequency where the reflection phase is zero is the resonant frequency of structure. At and around the resonance frequency, in a specific range, the surface impedance of respective structure is higher than or equal to characteristic impedance of free space, then reflection coefficient is $+1$, and hence the reflection phase is zero. The range lies between $+90^{\circ}$ to -90° region, where reflected waves interfere with the incident waves in-phase, so the respective electromagnetic band gap structure behave like an AMC in this region. In the lower and higher frequency regions, this structure exhibits similar reflection phase characteristics as those of a conventional perfect electric conductor (PEC) surface. Hence, any antenna element operating within AMC range can be directly

placed over the proposed design without being shorted. This enhances the radiation characteristics of the mounted antenna. The frequency of operation, AMC band width of three structures are extracted from reflection phase diagram shown in figure 5, and are depicted in Table II. The SEBG structure is exhibiting 1.22%, PSEBG is exhibiting 1.59%, less AMC band gap compared to MEBG model.

Table II: Comparison of AMC Band Gap of MEBG, SEBG and PSEBG Unit Cells

Parameter Name	MEBG	SEBG	PSEBG
Resonant frequency	2.5GHz	2.5GHz	2.5GHz
AMC band gap	404.2MHz	373.8MHz	364.4MHz
Fractional band gap	16.17%	14.95%	14.58%

High Impedance Region

High impedance region can be defined as a low loss reactive surface. At and around the resonance frequency, the impedance of MEBG, SEBG and PSEBG structures are exhibiting very high surface impedance as shown in figure 4. This property helps in development of low volume radiating antennas.

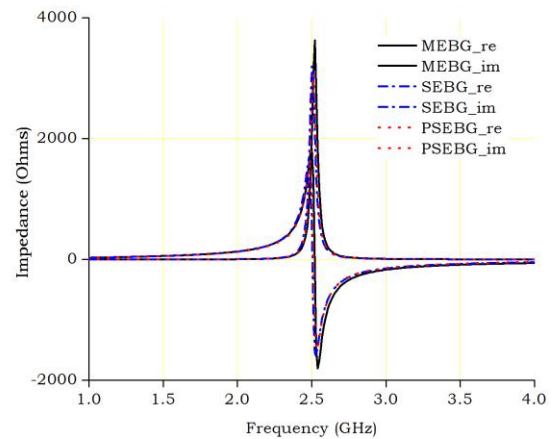


Fig. 6: High impedance nature of MEBG, SEBG and PSEBG unit cells.

Fbg Behavior Analysis

Under normal incidence, the EBG designs cannot be differentiated fully by their surface properties, so the FBG property of any EBG UC is obtained from its dispersion diagram. The simulation setup for measurement of FBG of electromagnetic band gap structure in FEM based simulator consists of a perfect matched layer (PML) boundary defined on the top of the UC model to intimate free space above the surface. Perfect magnetic conductors (PMC) and perfect electric conductors (PEC) boundaries are applied on four sides of the UC periodically [22,23]. The complete measurement setup for all three UC models are shown figure 7. In this paper $-X$ direction of propagation [24] is considered. The dispersion diagram (wave number versus frequency) contains first dispersion mode (maximum value of mode 1 determines the lower frequency limit of band gap or TM mode) and second dispersion mode (mode 2 or TE mode). The intersection of mode 2 with the light line determines the upper limit of frequency band gap. By examining the area between the lower and upper limits of band gap, forbidden band gap is obtained where surface propagation is inhibited.

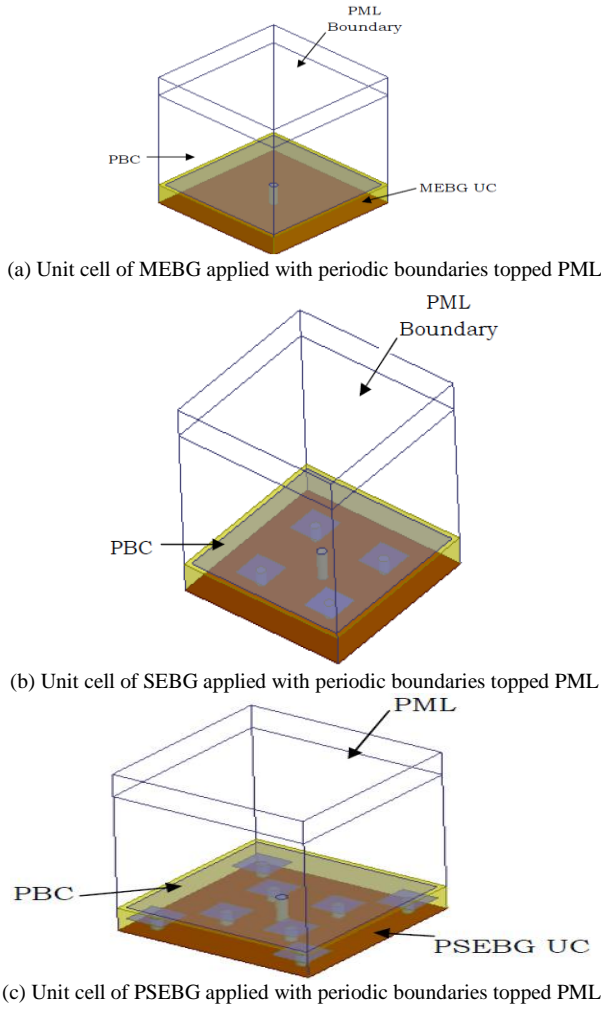
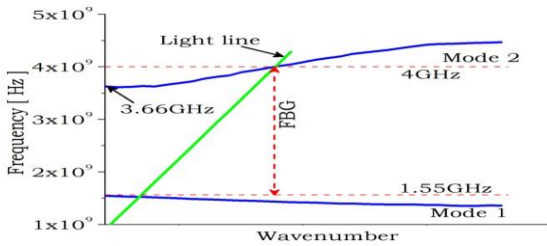
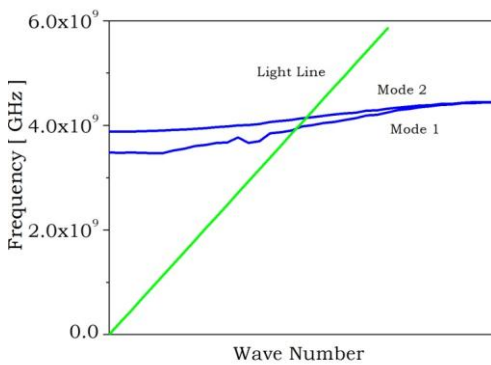


Fig. 7: FBG property measurement setup of MEBG, SEBG and PSEBG unit cells in FEM based simulator

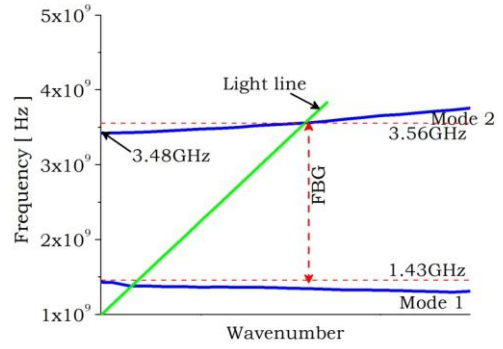


(a) Dispersion diagram of MEBG, represents FBG of 2.45GHz and leaky wave starting point of 3.66GHz

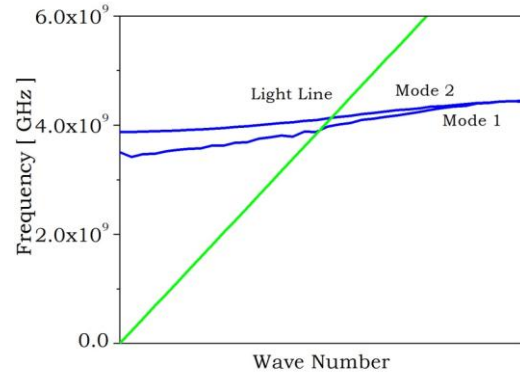


(b) MEBG without vertical conducting stub.

Fig. 8: Dispersion diagrams of MEBG model with and without vertical conducting stub.

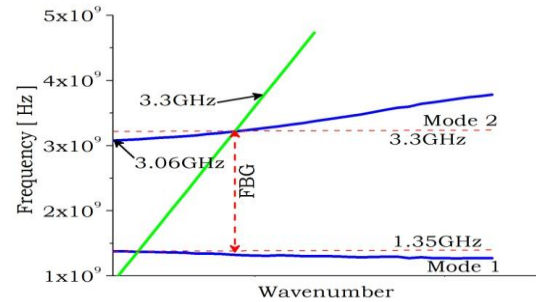


(a) Dispersion diagram of SEBG, represents FBG of 2.13GHz and leaky wave starting point of 3.48GHz

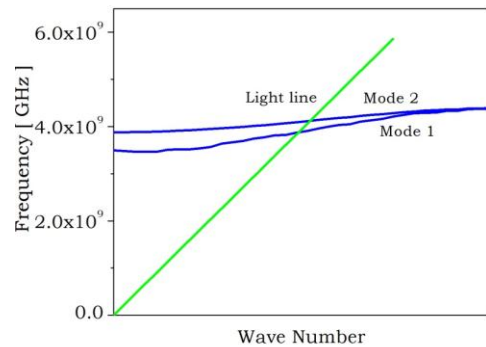


(b) SEBG without vertical conducting stub.

Fig. 9: Dispersion diagrams of SEBG model with and without vertical conducting stub



(a) Dispersion diagram of PSEBG, represents FBG of 1.95GHz and leaky wave starting point of 3.06GHz.



(b) PSEBG without vertical conducting stub.

Fig. 10: Dispersion diagrams of PSEBG model with and without vertical conducting stub.

Figure 8 to 10 are showing the dispersion diagrams of the three electromagnetic band gap architectures (MEBG, SEBG and PSEBG). This helps to understand the characteristics of propagation of EM waves and FBG property of respective UC. The dispersion diagram demonstrates that below the resonance frequency, the electromagnetic band gap structures supports TM waves, and they stay close to the light line, similar to the metal dielectric interface at lower frequencies. As the frequency slopes upward, the TM curve begins to bend, which indicates that the frequency is approaching resonance. At high frequencies, the proposed electromagnetic band gap structures supports TE surface waves. These TE waves start above the resonance frequency, slope upward along the light line but travel with less velocity, and start bending away from the light line to a small section after the resonance frequency. At the resonance frequency, the surface impedance of electromagnetic band gap structures is high, and group velocities for both TE and TM waves are very low, hence electromagnetic band gap structures are known as slow wave structures. Because the TM and TE bands never combine in this structure, the FBG can be defined as the range that starts from the TM band edge to the point of intersection of the light line with the TE band. The TE surface waves, lie above and left to the light line, in a short range of frequency, treated as radiative, leaky modes, these radiate efficiently into free space only when their phase matches with the phase of the plane wave along the interface. Figure 8(a) showing the FBG of MEBG, whose mode 1 is at 1.52GHz (TM mode edge) and mode 2 is at 4GHz (TE mode edge). The gap between mode 1 and mode 2 determines FBG is 2.45GHz. Figure 9(a) showing the FBG of SEBG is 2.13GHz, which is ranging from 1.43GHz to 3.56GHz. Figure 10(a) showing the FBG of PSEBG is 1.95GHz which is ranging from 1.43GHz to 3.56GHz. The leaky mode of MEBG is starting from 3.58GHz (figure 8(a)), SEBG is 3.48GHz (figure 9(a)) and PSEBG is 3.06GHz (figure 10(a)). Table III depicts the FBG of MEBG, SEBG and PSEBG, where fractional value of FBG is reducing from MEBG to PSEBG.

Table III: Comparison of FBG band gap of MEBG, SEBG and PSEBG Unit Cells

Parameter Name	MEBG	SEBG	PSEBG
Mode 1	1.55GHz	1.43GHz	1.35GHz
Mode 2	4GHz	3.56GHz	3.3GHz
FBG	2.45GHz	2.13GHz	1.95GHz
Fractional FBG	98%	85.2%	78%

During the FBG region, the electromagnetic band gap structures do not allow any surface currents, even radiative leaky TE waves to reach the edges of a radiating element that is lying over and parallel to electromagnetic band gap ground and operating within the FBG region. This avoids the interference of surface waves with radiated waves of antenna in the far field. This results, elimination of distortion or production of a smoother radiation pattern. Whereas Figures 8(b), 9(b) and 10(b) does not contain any forbidden band gap so these models are not suitable in suppression of surface wave propagation. So in next section we used MEBG, SEBG and PSEBG models with vertical conducting stubs between E plane array antenna to suppress the propagation of surface waves and avoid subway radiation.

4.Mitigation of Mutual Coupling in Array Antennas

Generally, the E-plane coupled antennas suffer from strong mutual coupling effect than the H-plane coupled antennas, because surface waves strongly propagate along the E-plane direction[25]. So, Initially E-plane coupled microstrip patch antenna array is designed on top face of FR4 substrate having thickness 3.2mm, while other face contains conducting ground as shown in figure

11. The results obtained in this model are taken as reference for comparison of results of MEBG, SEBG and PSEBG grounded models. The footprint of each microstrip patch has 32.55X26.85 mm² and conducting ground has dimensions of 110X55 mm² and both the patches are fed by co-axial cable matched to 50ohm. The thickness of substrate is made equal to height of electromagnetic band gap structures, so that electromagnetic band gap structures can be easily incorporated between array antennas in next stages of study and obtained results can be easily compared. The overall structure of microstrip patch antenna operate at 2.5GHz, this falls within the forbidden band gap of all three EBGs (described in table III). The edge to edge distance (denoted by 'S') between two patches is S=36.5mm. Results obtained are shown in figure 12, where coefficient of mutual coupling (S₂₁) between antenna elements is showing strong, of -23dB at 2.5GHz, return loss (S₁₁) of -20.25dB with an operational band width of 112MHz. The distance (S) between antenna elements is effecting the coefficient of coupling is investigated at different distance values, it was observed that the coefficient of coupling is reduced by increasing the distance (shown in figure 13) but volumetric size will increase.

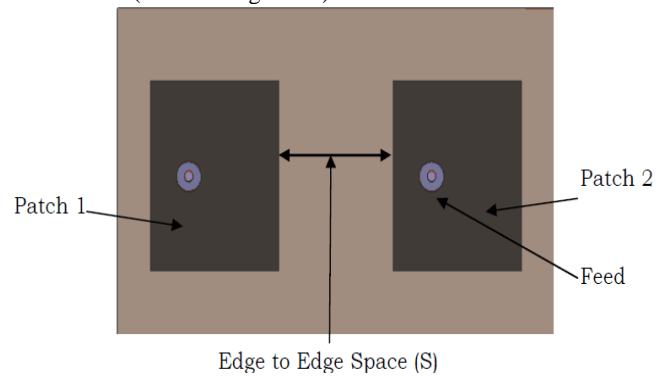


Fig. 11: E plane array antenna designed over FR4 substrate backed Conventional ground with a of thickness 3.2mm.

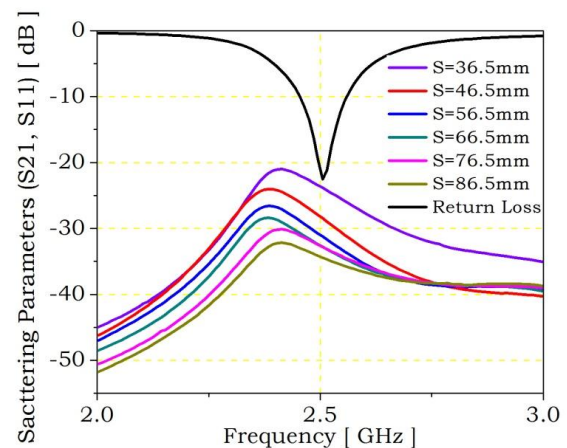


Fig. 12: Scattering parameters of conventional E plane array verses frequency

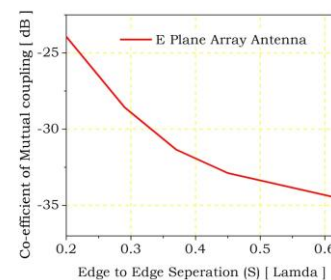


Fig. 13: Co-efficient of mutual coupling between array antenna for E plane direction.

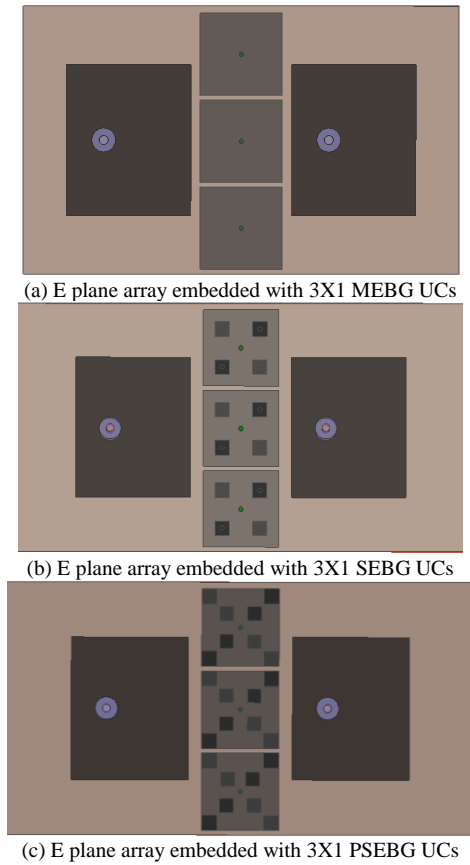


Fig. 14: E plane array antenna embedded by MEBG, SEBG and PSEBG UCs of 3X1 array.

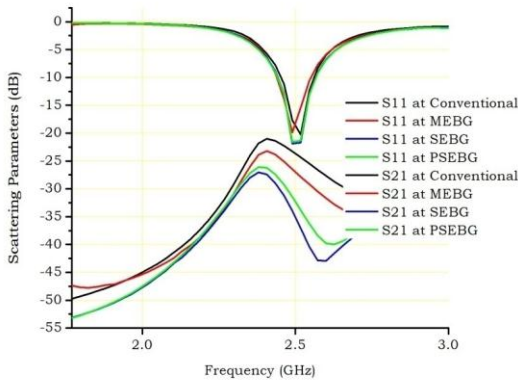


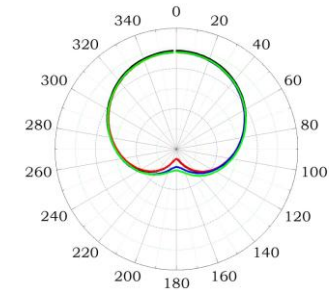
Fig. 15: Scattering parameters verses frequency, when E plane array embedded by MEBG, SEBG and PSEBG UCs of 3X1 array.

The effectiveness of MEBG, SEBG or PSEBG on mutual coupling between array antennas is investigated in this section by inserting 3X1 array of electromagnetic band gap unit cells between an antenna elements. The complete arrangement show in figure 14(a), 14(b), 14(c). For comparative analysis, the antenna size, substrate properties, distance between antenna elements is maintained identical in all cases of study. The complete dimensions of the four models are presented in table III. First of all, the MEBG UCs are introduced between array elements (figure 14(a)), the level of mutual coupling (S_{21}) is reduced to -28dB at 2.4925GHz, return loss (S_{11}) of -19.45dB with an operational band width of 112.9MHz, shown in figure 15 (black colour). In this case, the level of coefficient of mutual coupling is reduced by 5dB compared with conventional array design. Next the MEBG UCs are replaced by SEBG UCs between array elements (figure 14(b)), then the level of mutual coupling (S_{21}) is reduced to -35dB at 2.5GHz, return loss (S_{11}) of -21.8dB with an operational band width of 125.4MHz, shown in figure 15 (blue colour). In this case,

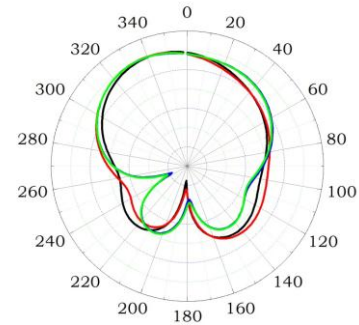
the level of coefficient of coupling is reduced by 12dB compared with conventional array design. Lastly, the PSEBG UCs are introduced then the level of mutual coupling (S_{21}) is reduced to -33dB at 2.5GHz, return loss (S_{11}) of -21.5dB with an operational band width of 130MHz, shown in figure 15 (red colour). In this case, the level of coefficient of coupling is reduced by 10dB compared with conventional array design.

Table IV: Comparison of parameters and results obtained during simulation of an array antenna over the conventional, MEBG, SEBG and PSEBG grounds

Parameter	Conventional Ground	MEBG Ground	SEBG Ground	PSEBG Ground
Patch	32.55X26.85 mm ²	32.55X26.85 mm ²	32.55X26.85 mm ²	32.55X26.85 mm ²
Gap	36.5mm	36.5mm	36.5mm	36.5mm
Ground size	110X55 mm ²	110X55 mm ²	110X55 mm ²	110X55 mm ²
Substrate thickness	3.2mm	3.2mm	3.2mm	3.2mm
Operating frequency	2.5GHz	2.5GHz	2.5GHz	2.5GHz
Return loss	-20.25dB	-19.45dB	-21.8dB	-21.5dB
Band width	112 MHz	112.9 MHz	125.4 MHz	130 MHz
Radiating efficiency (%)	60	70	75	75
Coefficient of coupling	-23dB	-28dB	-35dB	-33dB



(a) H Plane pattern of array antenna ($\Phi=0$ degree)



(b) E Plane pattern of array antenna ($\Phi=90$ degree)

Fig. 16: Radiation (Gain) pattern of E plane array antenna

Figure 16(a), 16(b) showing the H, E plane radiation (gain) pattern of microstrip patch array antennas at 2.5GHz, over the conventional, MEBG, SEBG and PSEBG ground. It is observed that the radiation pattern of array antenna has no effect of three electromagnetic band gap structures, and occurred a slight enhancement in gain along with improvement in isolation. The radiation efficiency of array antenna also improved by the introduction of three electromagnetic band gap structures. The radiation efficiency of conventional array design (figure 11) exhibiting 60%, with MEBG (figure 14(a)) array antenna has 70%, SEBG (figure 14(b)) and PSEBG (figure 14(c)) has 75%. The radiation efficiency improvement of 15% achieved by the SEBG and PSEBG introduction when compared with

conventional design and improvement of 10% when compared with MEBG. Furthermore, various methodologies available in literature and its results are presented in table V, for better comparison of proposed model results.

Table V: Comparison of proposed model results with literature results

Ref. No.	Method	Size of array (mm ²)	Frequency (GHz)	Space between patches	Isolation level (dB)
[18]	EBG with Multilayer substrate	130X130	3	40mm	10
[14]	Uniplanar EBG	78.3X78.3	5.75	26mm	10
[15]	EBG	Not given	8	Not given	5
[12]	DGS	63.5X40	9.2	8.6mm	16.50
Reference	MEBG	18.5X55.5	2.5	36.5mm	5
Reference	SEBG	18.5X55.5	2.5	36.5mm	12
Reference	PSEBG	18.5X55.5	2.5	36.5mm	10

5. Conclusion

In this paper, two new electromagnetic band gap structures are developed from MEBG structure and named as SEBG and PSEBG structure. The unique (FBG and AMC) properties of SEBG and PSEBG are determined using FEM based simulator and obtained results are compared with reference MEBG model. The size of FBG is reducing from MEBG to PSEBG. The influence of vertical conducting stub on FBG property is studied and understood that FBG property is zero in the absence of stubs in electromagnetic band gap structures. Also studied the coefficient of mutual coupling between antenna elements by the incorporating MEBG, SEBG and PSEBG structures. The simulation results obtained are showing that SEBG and PSEBG structures are reducing the coefficient of mutual coupling compared to MEBG. Mutual coupling reduction of 12dB is achieved by new SEBG model.

References

- [1] Kamfelt C, Hallbjörner P, Zirath H & Alping A, "High gain active microstrip antenna for 60-GHz WLAN/WPAN applications", *IEEE Trans. Microwave Theory Tech.*, (2006), pp.2593–2603.
- [2] Ludwig A, "Mutual coupling, gain and directivity of an array of two identical antennas", *IEEE Trans. Antennas Propag.*, Vol.24, No.6, (1976), pp.837–841.
- [3] Ngai EC & Blejer DJ, "Mutual coupling analyses for small GPS adaptive arrays", *IEEE Antennas and Propagation Society International Symposium*, Vol.4, (2001).
- [4] Van Trees HL, *Optimum Array Processing, Part IV of Detection, Estimation, and Modulation Theory*, Wiley-Interscience, (2002).
- [5] Kildal PS, "Artificially soft and hard surfaces in electromagnetics and their application to antenna design", *23rd European Microwave Conference*, (1993).
- [6] Rajo-Iglesias E, Quevedo-Teruel O & Inclan-Sanchez L, "Planar soft surfaces and their application to mutual coupling reduction" *IEEE Transactions on Antennas and Propagation*, Vol.57, No.12, (2009), pp.3852–3859.
- [7] Buell K, Mosallaei H & Sarabandi K, "Electromagnetic metamaterial insulator to eliminate substrate surface waves", *IEEE Antennas and Propagation Society International Symposium*, Vol.2A, (2005), pp.574–577.
- [8] Bait-Suwailam MM, Siddiqui OF & Ramahi OM, "Mutual coupling reduction between microstrip patch antennas using slotted-complementary split-ring resonators", *IEEE Antennas Wireless Propag. Lett.*, Vol.9, (2010), pp.876–878.
- [9] Guha D, Biswas S, Biswas M, Siddiqui JY & Antar, YMM, "Concentric ring-shaped defected ground structures for microstrip applications", *IEEE Antennas and Wireless Propagation Letters*, Vol.5, No.1, (2006), pp.402–405.
- [10] Chiu CY, Cheng CH, Murch RD & Rowell CR, "Reduction of mutual coupling between closely-packed antenna elements", *IEEE Transactions on Antennas and Propagation*, Vol.55, No.6, (2007), pp.1732–1738.
- [11] Habashi A, Naurinia J & Ghabadi C, "A rectangular defected ground structure for reduction of mutual coupling between closely spaced microstrip antennas", *Proc. 20th Iranian Conf. Elect. Eng.*, (2012), pp.1347–1350.
- [12] Sievenpiper D, Zhang L, Broas RFJ, Alexopolous, NG & Yablonovitch E, "High impedance electromagnetic surfaces with a forbidden frequency band", *IEEE Transactions on Microwave Theory and Techniques*, Vol.47, No.11, (1999).
- [13] Farahani H, Veysi M, Kamyab M & Tadjalli A, "Mutual coupling reduction in patch antenna arrays using a UC-EBG superstrate", *IEEE Antennas Wireless Propag. Lett.*, Vol.9, (2010), pp.57–59.
- [14] Expósito-Domínguez G, Fernández-González JM, Padilla P & Sierra-Castaner M, "New EBG solutions for mutual coupling reduction", *Proc. 6th EuCAP*, (2011), pp.2841–2844.
- [15] Yang F & Rahmat-Samii Y, "Microstrip antennas integrated with electromagnetic band-gap (EBG) structures: A low mutual coupling design for array applications", *IEEE Transactions on Antennas and Propagation*, Vol.51, No.10, (2003), pp.2936–2946.
- [16] Simovski CR & Sochava AA, "High-impedance surfaces based on self-resonant grids. Analytical modelling and numerical simulations", *Progress In Electromagnetics Research*, Vol.43, (2003), pp.239–256.
- [17] Rajo-Iglesias E, Quevedo-Teruel O & Inclan-Sanchez L, "Mutual coupling reduction in patch antenna arrays by using a planar EBG structure and a multilayer dielectric substrate", *IEEE Transactions on Antennas and Propagation*, Vol.56, No.6, (2008), pp.1648–1655.
- [18] Fan MY, Hu R, Feng ZH, Zhang XX & Hao Q, "Advance in 2D-EBG research", *Journal of Infrared Millimeter Waves*, Vol.22, No. 2, (2003).
- [19] Lin BQ, Zheng QR & Yuan NC, "A novel spiral high impedance surface structure for size reduction", *Microwave and Optical Technology Letters*, Vol.49, No 9, (2007).
- [20] Pal Reddy S, "Wide band electromagnetic band gap structures, analysis applications to antennas", *PhD Dissertation*, (2015).
- [21] Rahman M & Stuchly MA, "Transmission line-periodic circuit representation of planar microwave photonic bandgap structures", *Microwave Optical Tech. Lett.*, Vol.30, No.1, (2001), pp.15–19.
- [22] Grbic A & Eleftheriades G, "Periodic analysis of a 2-D negative refractive index transmission line structure", *IEEE Transactions on Antennas and Propagation*, Vol.51, No.10, (2003), pp.2604–2611.
- [23] Eleftheriades G & Balmmain KG, "Negative Refraction Metamaterials: Fundamental Principles and Applications", New York: Wiley-IEEE Press, (2005).
- [24] Joannopoulos JD, Johnson SG, Winn JN & Meade RD, *Photonic Crystals: Molding the Flow of Light*, 2nd edition, Princeton University Press, (2008).
- [25] Raimopno L, Paulis FD & Orlandi A, "A simple and efficient design procedure for planar electromagnetic bandgap structures on printed circuit boards", *IEEE Trans. Electromagnetic. Compat.* (2011), pp.482–490.